

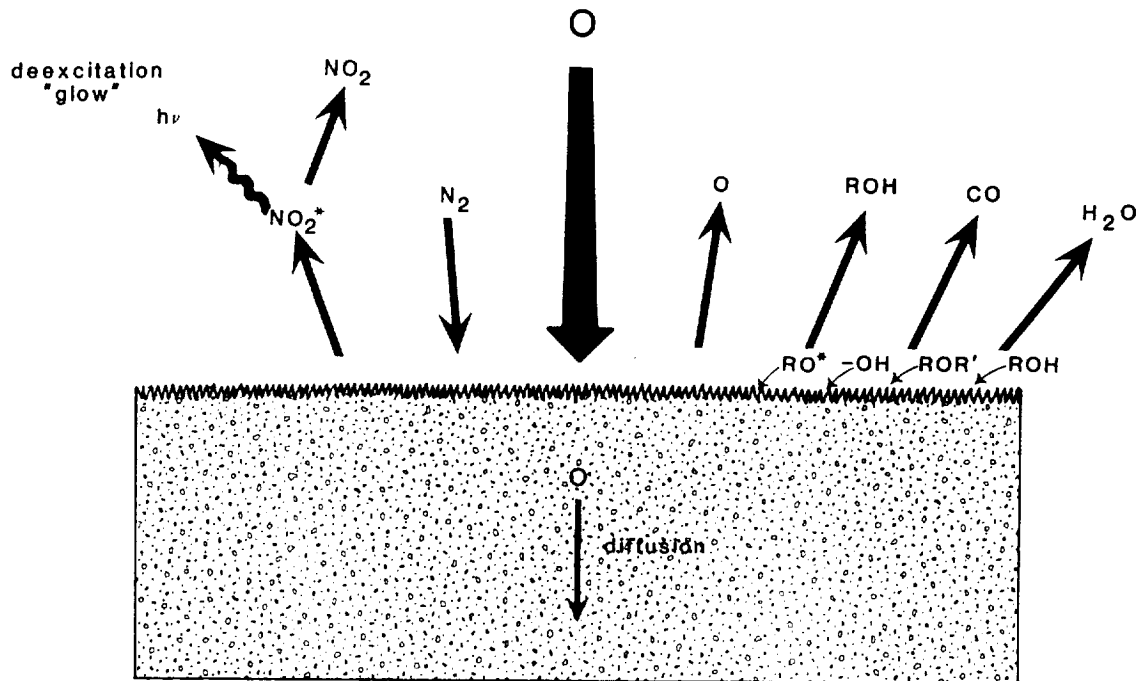
ATOMIC OXYGEN EFFECTS ON MATERIALS *

Bruce A. Banks, NASA Lewis Research Center
Sharon K. Rutledge, NASA Lewis Research Center
Joyce A. Brady, Sverdrup Technology, Inc.
Cleveland, Ohio
James E. Merrow, Ohio University
Athens, Ohio

*Original photographs not available at time of publication.

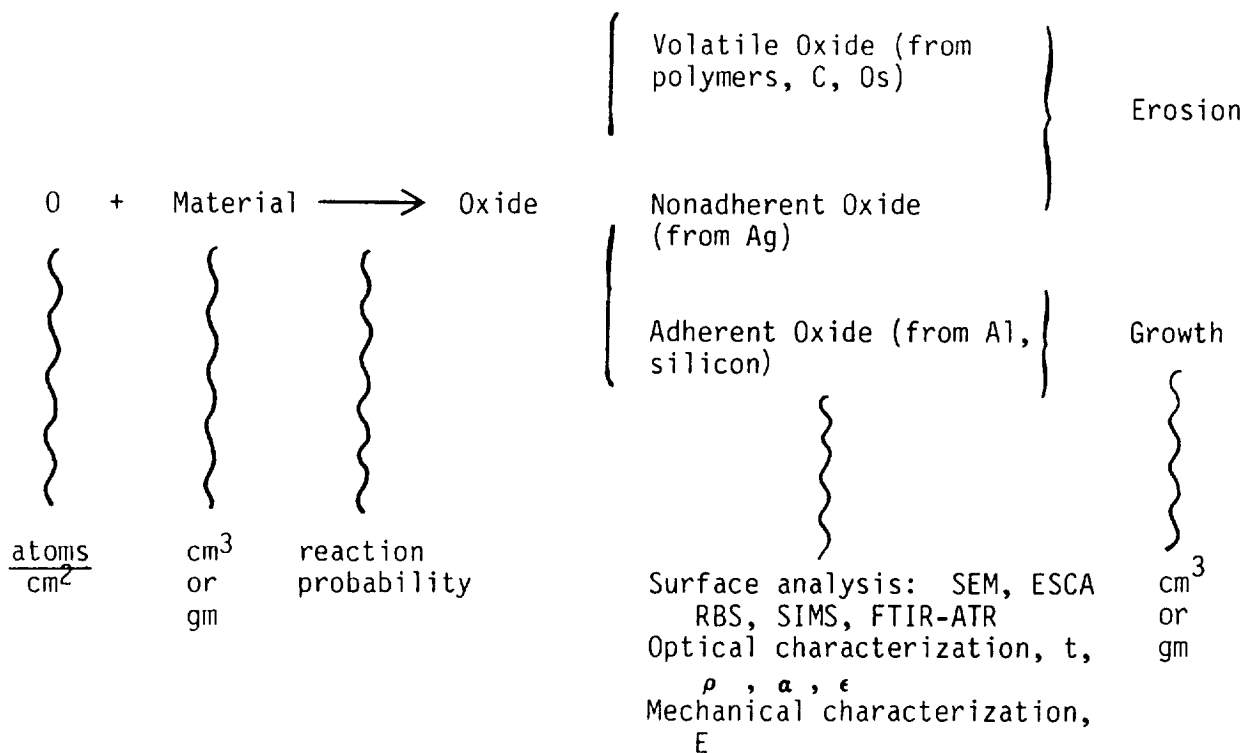
ATOMIC OXYGEN SURFACE INTERACTION PROCESSES

Atomic oxygen with an energy level of 4 - 5 eV may initiate numerous chemical and physical events on the surface it impacts. The atomic oxygen may simply be scattered or it may chemically react with nitrogen, also incident upon the surface, to form nitrous oxide in an excited state, which can de-excite to produce a glow. If atomic oxygen reacts with an organic material, volatile fragments, such as short chain oxidation products, may leave the surface. The surface may also be populated with excited state fragments, radicals, or polymeric molecules with oxygen-containing functionalities. The oxygen may also, as in the case of silver, diffuse into the bulk of the material.



QUANTIFICATION OF ATOMIC OXYGEN EFFECTS ON MATERIALS

The quantification of atomic oxygen interaction with materials has generally been performed by measuring the atomic oxygen flux and multiplying it by the duration of exposure, which results in an atomic oxygen fluence in terms of atoms per square centimeter. The material is usually measured in terms of weight or volume, and the probability that oxygen will react with the material can be measured (for some materials) in terms of reaction probability. The chemistry of the surface which is reacting with the incident oxygen may cause the formation of volatile oxides from polymers, carbon, and osmium; or oxides which are not adherent and tend to spall, as in the case of silver, may form. Both of these types of surface oxides contribute to net erosion of the surface. If the surface material being impinged by atomic oxygen forms an adherent oxide, such as aluminum forming aluminum oxide or silicones forming silicon dioxide on the surface, then the surface may grow. The chemistry of the remaining or reacted surface may be analyzed by surface analysis, optical characterization, and mechanical characterization (in terms of modulus and elasticity). If net erosion of the material surface occurs, the volume or mass loss is quantified and used to calculate an erosion or recession per incident oxygen atom, generally in units of cubic centimeters per incident oxygen atom.



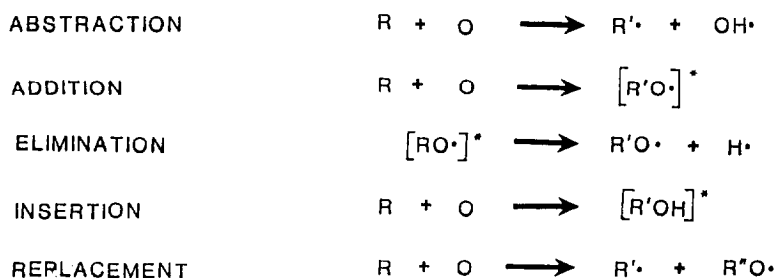
ATOMIC OXYGEN REACTION PROBABILITIES

The probability of atomic oxygen reacting with a given material can be calculated for those materials which form known or simple oxides. Using erosion yield numbers from space tests, one finds that atomic oxygen has a rather low probability (approximately 13%) of reacting with carbon to form carbon monoxide. However, in the case of silver, a very high fraction of the incident atomic oxygen reacts with the silver to form silver oxide. Because the silver oxide may tend to shield from further oxidation or be a catalyst surface for recombination of atomic oxygen on the surface, the reaction probability for silver is expected to drop as the degree of oxidation on the surface becomes higher.

<u>MATERIAL</u>	<u>EROSION YIELD, cm³/atom</u>	<u>REACTION PROBABILITY, %</u>
Carbon	1.2×10^{-24}	13
Silver	10.7×10^{-24}	62

ATOMIC OXYGEN REACTION MECHANISMS WITH POLYMERS

Various mechanisms have been suggested for the reactions of atomic oxygen with polymers based on studies with simple organic compounds. Basic processes are labeled as abstraction, addition, elimination, insertion, and replacement reactions. Abstraction is the process by which atomic oxygen "abstracts" an atom, such as hydrogen, from the compound. "Addition" describes the process by which an oxygen atom adds or attaches itself to an organic compound. This has been observed for the reaction with a typical alkene, and the initial product is a vibrationally excited molecule which can then undergo "elimination" of a hydrogen atom. Atomic oxygen has also been observed to "insert" between two bound atoms, such as carbon and hydrogen in an organic molecule. "Replacement" is the mechanism by which an oxygen atom attaches to the molecule and a portion of the original molecule departs (usually as a radical). Oxygen, in effect, replaces a group originally present on the molecule producing an alkoxy radical and an alkyl radical.



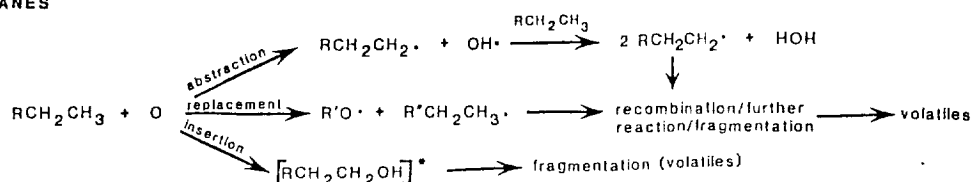
ATOMIC OXYGEN REACTION MECHANISMS

Reactions of atomic oxygen with polymers have been shown to occur by various mechanisms. Under thermal energy conditions, it is known that ground state atomic oxygen $O(^3P)$ abstracts hydrogen from saturated organic molecules. Singlet atomic oxygen $O(^1D)$ at thermal energy, inserts into C-H bonds in saturated organic molecules to form alcohols. Another suggested mechanism is replacement to form alkyl radicals and alkoxy radicals. These primary reaction products undergo further reactions which lead to fragmentation of the reactants. The fragmentation products form weakness of bonds. Under high vacuum conditions, moderate molecular weight oligomers and fragments are volatile.

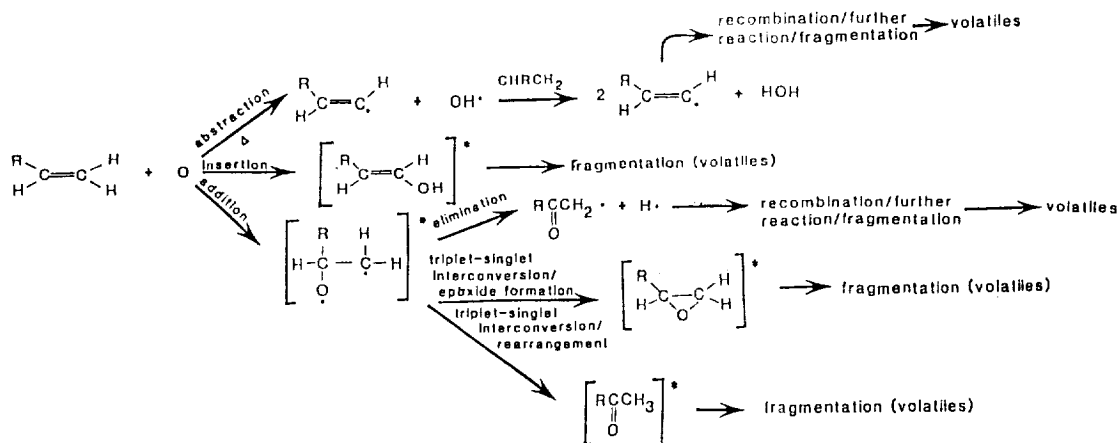
Unsaturated organic molecules show different pathways leading to formation of fragments and volatiles. $O(^3P)$ adds to carbon-carbon double bonds, forming metastable triplet biradical intermediates which can undergo further reaction to form epoxide, aldehyde, and ketone products. The favored pathway for the reaction of the triplet biradical is hydrogen elimination to form a carbonyl-containing radical. $O(^1D)$ inserts into C-H bonds in alkenes and the resulting metastable species undergoes further reaction. At high temperatures, hydrogen abstraction may compete with O atom insertion.

It is important to note that at high energy, $O(^3P)$ acts similarly to $O(^1D)$ and it is more difficult to distinguish between them.

ALKANES



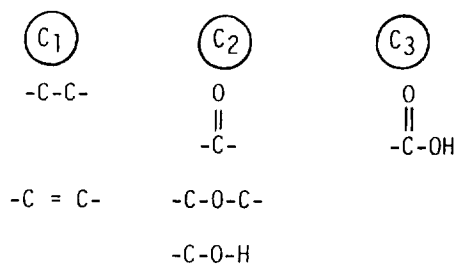
ALKENES



ESCA ANALYSIS OF POLYETHYLENE SURFACE

Surface chemical analysis by means of ESCA has been performed on polyethylene surfaces exposed to atomic oxygen in low Earth orbit. Such analyses performed by Coulter, Liang, Chung, Smith, and Gupta have indicated that olefin formation is not an important process in atomic oxygen interaction with polyethylene.

	C ₁	C ₂	C ₃	O
Theoretical	100.0	--	--	--
Control	99.2	--	--	0.8
Exposed	81.5	4.5	3.1	9.9



EROSION YIELDS OF VARIOUS MATERIALS EXPOSED TO
ATOMIC OXYGEN IN LOW EARTH ORBIT

The erosion yields of various materials exposed to atomic oxygen are listed along with their sources for all the references known to the authors at the present time.

MATERIAL	EROSION YIELD, $\times 10^{-24}$ cm ³ /ATOM	REFERENCE
Aluminum (150 Å)	0.0	1
Aluminum-coated Kapton	0.01	2
Aluminum-coated Kapton	0.1	2
Al ₂ O ₃	<0.025	3
Al ₂ O ₃ (700 Å) on Kapton H	<0.02	4
Apiezon grease 2 μm	>0.625	5
Aquadag E (graphite in an aqueous binder)	1.23	6
Carbon	1.2	7, 1, 8, 9
Carbon (various forms)	0.9 - 1.7	10
Carbon/Kapton 100XAC37	1.5	11
401-C10 (flat black)	0.30	12

MATERIAL	EROSION YIELD, x 10 ⁻²⁴ cm ³ /ATOM	REFERENCE
Chromium (123 Å)	partially eroded	14
Chromium (125 Å) on Kapton H	0.006	15, 16
Copper (bulk)	0.0	17
Copper (1,000 Å) on sapphire	0.007	15, 16
Copper (1,000 Å)	0.0064	14
Diamond	0.021	17
Electrodag 402 (silver in a silicone binder)	0.057	6
Electrodag 106 (graphite in an epoxy binder)	1.17	6
Epoxy	1.7	10, 16
Fluoropolymers:		
FEP Kapton	0.03	18
Kapton F	<0.05	6
Teflon, FEP	0.037	5
Teflon, FEP	<0.05	10

MATERIAL	EROSION YIELD, x 10 ⁻²⁴ cm ³ /ATOM	REFERENCE
Teflon, TFE	<0.05	10, 6
Teflon, FEP and TFE	0.0 and 0.2	15, 19
Teflon, FEP and TFE	0.1	15
Teflon	0.109	19
Teflon	0.5	15
Teflon	0.03	15
Teflon	<0.03	9
Gold (bulk)	0.0	17
Gold	appears resistant	20
Graphite Epoxy:		
1034 C	2.1	10
5208/T300	2.6	10
GSFC Green	0.0	1
HOS-875 (bare and preox)	0.0	1
Indium Tin Oxide	0.002	15, 16
Indium Tin Oxide/Kapton (aluminized)	0.01	2
Iridium Film	0.0007	17

MATERIAL	EROSION YIELD, $\times 10^{-24}$ cm ³ /ATOM	REFERENCE
Lead	0.0	1
Magnesium	0.0	1
Magnesium Fluoride on glass	0.007	15, 16
Molybdenum (1,000 Å)	0.0056	4
Molybdenum (1,000 Å)	0.006	15, 16
Molybdenum	0.0	1
Mylar	3.4	10
Mylar	2.3	15, 19
Mylar	3.9	15, 19, 9
Mylar	1.5 - 3.9	15
Mylar A	3.7	18
Mylar A	3.4	21, 6
Mylar A	3.6	6
Mylar D	3.0	6
Mylar D	2.9	21
Mylar with Antiox	heavily attacked	22
Nichrome (100 Å)	0.0	1

MATERIAL	EROSION YIELD, $\times 10^{-24}$ cm ³ /ATOM	REFERENCE
Nickel film	0.0	17
Nickel	0.0	8
Niobium film	0.0	17, 1
Osmium	0.026	10
Osmium	heavily attacked	20
Osmium (bulk)	0.314	17
Parylene, 2.5 μm	eroded away	22
Platinum	0.0	1
Platinum	appears resistant	20
Platinum film	0.0	17
Polybenzimidazole	1.5	10, 7
Polycarbonate	6.0	8
Polycarbonate resin	2.9	17
Polyester - 7% Poly-silane/93% Polyimide	0.6	10
Polyester	heavily attacked	10, 22
Polyester with Antiox	heavily attacked	10, 22
Polyester (Pen-2,6)	2.9	23
Polyethylene	3.7	10, 21, 16, 15

MATERIAL	EROSION YIELD, x 10 ⁻²⁴ cm ³ /ATOM	REFERENCE
Polyethylene	3.3	18, 6
Polyimides:		
BJPIPSX-9	0.28	23
BJPIPSX-9	0.071	24
BJPIPSX-11	0.56	23
BJPIPSX-11	0.15	24
BTDA-Benzidene	3.08	23
BTDA-DAF	2.82	23
BTDA-DAF	0.8	24
BTDA-mm-DD502	2.29	23
BTDA-mm-MDA	3.12	23
BTDA-pp-DABP	2.91	23
BTDA-pp-DABP	3.97	23
Kapton (black)	1.4 - 2.2	15, 12
Kapton (TV blanket)	2.0	15
Kapton (TV blanket)	2.04	19
Kapton (OSS - 1 blanket)	2.55	15
Kapton (OSS - 1 blanket)	2.5	15

MATERIAL	EROSION YIELD, x 10 ⁻²⁴ cm ³ /ATOM	REFERENCE
Kapton H	3.0	10, 15, 19, 4, 6, 9
Kapton H	2.4	15, 19
Kapton H	2.7	15, 18
Kapton H	1.5 - 2.8	15
Kapton H	2.0	18
Kapton H	3.1	18
ODPA-mm-DABP	3.53	23
PMDA-pp-DABP	3.82	23
PMDA-pp-MDA	3.17	23, 24
PMDA-pp-ODA	4.66	23
Polymethylmethacrylate	3.1	16
25% Polysiloxane, 45% Polyimide	0.3	10
25% Polysiloxane-Polyimide	0.3	9
Polystyrene	1.7	10, 16, 9
Polysulfone	2.4	10, 16
Polyvinylidene Fluoride	0.6	9

MATERIAL	EROSION YIELD, $\times 10^{-24} \text{ cm}^3/\text{ATOM}$	REFERENCE
Pyrrone:		
PMDA-DAB	2.5	23
S-13-GLO, white	0.0	12
SiO ₂ (650 Å) on Kapton H	0.00103	4
SiO _x /Kapton (aluminized)	0.01	2
Silicones:		
DC1-2577	0.055	21
DC1-2755-coated Kapton	0.05	15
DC1-2775-coated Kapton	<0.5	15
DC6-1104	0.0515	20
Grease 60 μm	intact but oxidized	25
RTV-560	0.443	21
RTV-615 (black, conductive)	0.0	20
RTV-615 (clear)	0.0625	5
RTV-670	0.0	1

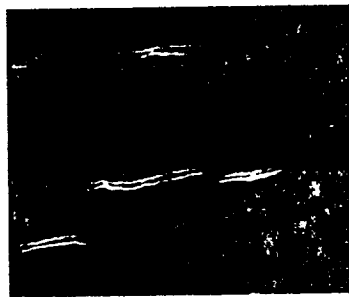
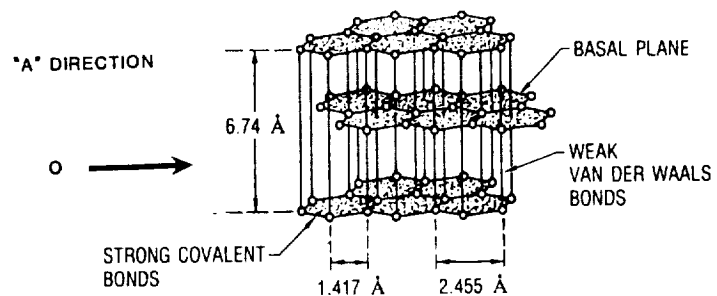
MATERIAL	EROSION YIELD, $\times 10^{-24} \text{ cm}^3/\text{ATOM}$	REFERENCE
RTV-S695	1.48	11
RTV-3145	0.128	1
T-650-coated Kapton	<0.5	15
Siloxane Polyimide (25% Sx)	0.3	7
Siloxane Polyimide (7% Sx)	0.6	7
Silver	10.5	5
Tantalum	appears resistant	20
Tedlar	3.2	10
Tedlar (clear)	1.3 and 3.2	15
Tedlar (clear)	3.2	18, 6
Tedlar (white)	0.4 and 0.6	15
Tedlar (white)	0.05	15
TiO ₂ , (1,000 Å)	0.0067	5
Trophet 30 (bare and preox)	0.0	1
Tungsten	0.0	8
Tungsten Carbide	0.0	8
YB-71 (ZOT)	0.0	7

EROSION YIELD TABLE
REFERENCES

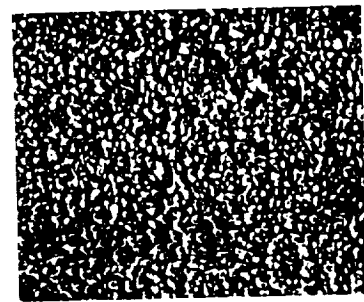
1. Marshall Space Flight Center
2. Smith, K. A. Evaluation of oxygen interaction with materials (E01M) - STS-8 atomic oxygen effects. AIAA-85-7021. November, 1985.
3. Durcanin, J. T., and Chalmers, D. R. The definition of low earth orbital environment and its effect on thermal control materials. AIAA-87-1599. June, 1987.
4. Banks, B. A., Mirtich, M. J., Rutledge, S. K., and Nagra, H. K. Protection of solar array blankets from attack by low earth orbital atomic oxygen. 18th IEEE Photovoltaic Specialists Conference. October, 1985.
5. Purvis, C. K., Ferguson, D. C., Snyder, D. B., Grier, N. T., Staskus, J. V., and Roche, J. C. Environmental interactions considerations for space station and solar array design. Preliminary - December, 1986.
6. Visentine, J. T., Leger, L. G., Kuminecz, J. F., and Spiker, I. K. NASA JSC STS-8 atomic oxygen effects experiment. AIAA 23rd Aerospace Sciences Meeting. January, 1985.
7. Langley Research Center
8. University of Alabama at Huntsville
9. Coutler, D. R., Liang, R. H., Chung, S. H., Smith, K. O., and Gupta, A. O-atom degradation mechanisms of materials. Taken from Proceedings of NASA Workshop on Atomic Oxygen Effects. June 1, 1987, p. 42.
10. Leger, L. G., Santos-Mason, B., Visentine, J. T., and Kuminecz, J. F. Review of LEO flight experiments. Proceedings on the NASA Workshop on Atomic Oxygen Effects. November, 1986, p. 6.
11. British Aerospace
12. Whitaker, A. F. LEO atomic oxygen effects on spacecraft materials.
13. Martin Marietta
14. Lewis Research Center
15. Leger, L. J., Spiker, I. K., Kuminecz, J. F., Ballentine, T. J., and Visentine, J. T. STS Flight 5 LEO effects experiment - Background description and thin film results. AIAA-83-2631-CP. October, 1983.
16. Jet Propulsion Laboratory
17. Gregory, J. C. Interaction of hyperthermal atoms on surfaces in orbit: The University of Alabama Experiment. Proceedings of the NASA Workshop on Atomic Oxygen Effects. November, 1986, p. 31.
18. Leger, L. J., Visentine, J. T., and Kuminecz, J. F. Low earth orbit.
19. Leger, L. J. Oxygen atom reaction with shuttle materials at orbital altitudes - Data and experiment status. AIAA-83-0073. January, 1983.
20. Goddard Space Flight Center
21. Johnson Space Center
22. Washington University
23. Slomp, W. S., Santos-Mason, B., Bykes, G. F., Jr. and Witte, W. S., Jr. Effects of STS-8 atomic oxygen exposure on composites, polymeric films and coatings. AIAA-85-0421. January, 1985.
24. Santos, B. The dependence of atomic oxygen resistance on polyimide structures. (Preliminary results of STS-8). NASA Headquarters. January 23-24, 1984.
25. Aerospace Corporation

ATOMIC OXYGEN ATTACK OF PYROLYTIC GRAPHITE, A-PLANE (STS-8)

Atomic oxygen attack of both polymers and graphite tends to cause the development of microscopic cone-like surface structures. Such cone-like structures develop in the "A" or prismatic plane direction for pyrolytic graphite. Pronounced structures are evident for RAM-only attack. However, only minor roughening occurs under sweeping atomic oxygen incidence.



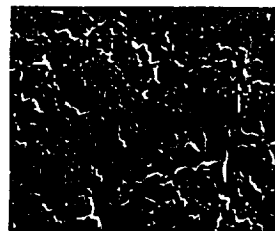
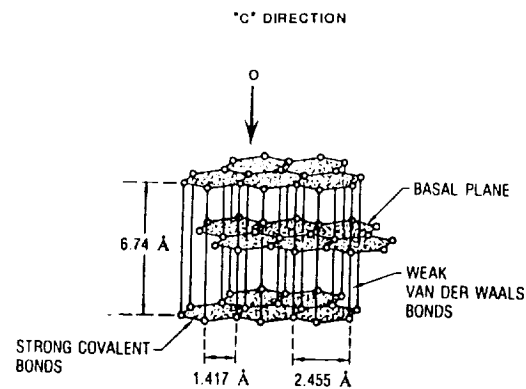
1 μm preflight



1 μm postflight

ATOMIC OXYGEN ATTACK OF PYROLYTIC GRAPHITE, C-PLANE (STS-8)

Atomic oxygen bombardment of the C-plane or basal plane of graphite also causes the formation of surface texture, even though there is no apparent rationale for such development with respect to differential erosion yields for amorphous compared to graphitic regions, as may occur in polymeric materials such as Kapton, Mylar, and fluoropolymers.



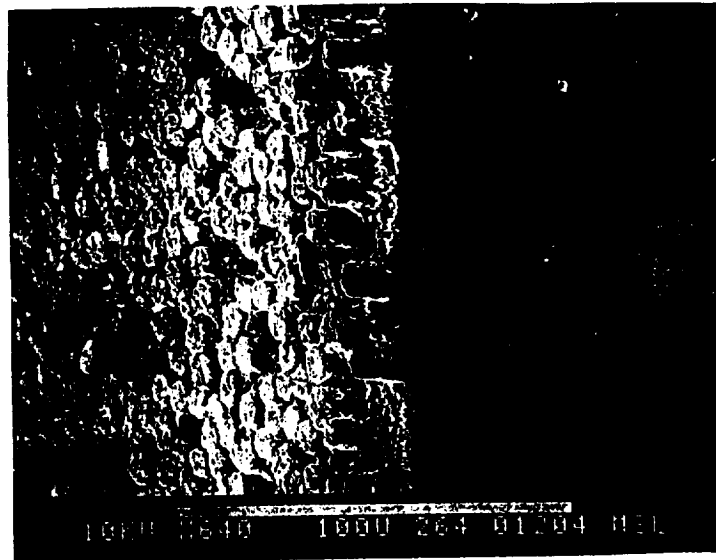
1 μm PREFLIGHT



1 μm POSTFLIGHT

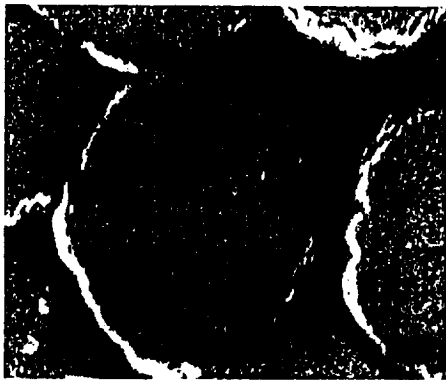
CARBON FIBERS IN EPOXY MATRIX EXPOSED TO ATOMIC OXYGEN (STS-8)

Differences in erosion yield for graphite or carbon fiber epoxy composites result in exposure of the carbon fibers because of more accelerated erosion of the epoxy matrix material.



PAN FIBERS IN EPOXY EXPOSURE TO ATOMIC OXYGEN (STS-8)

PAN fibers (polyacrylonitrile derived) also develop a cone-like microscopic surface morphology. In fact, pitch and PAN based fibers both develop a cone-like morphology upon RAM attack by atomic oxygen. In general, all bulk materials with volatile oxidation products tend to develop cone-like surface morphology upon RAM attack.



PREFLIGHT

1 um

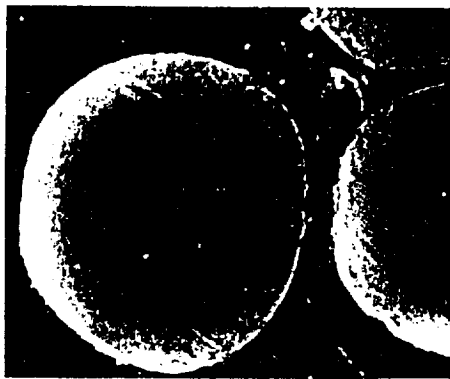


POSTFLIGHT

1 um

KEVLAR POLYIMIDE FIBERS IN EPOXY EXPOSURE TO ATOMIC OXYGEN (STS-8)

Kevlar polyimide fibers develop a surface texture very similar to Kapton polyimide.



2 um

PREFLIGHT

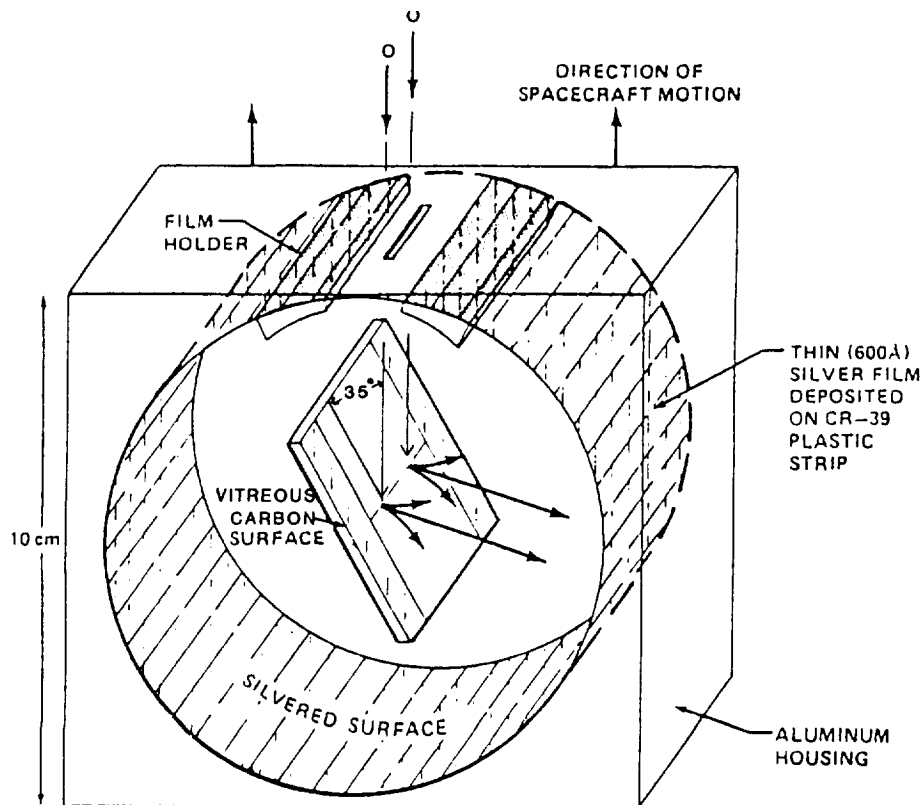


2 um

POSTFLIGHT

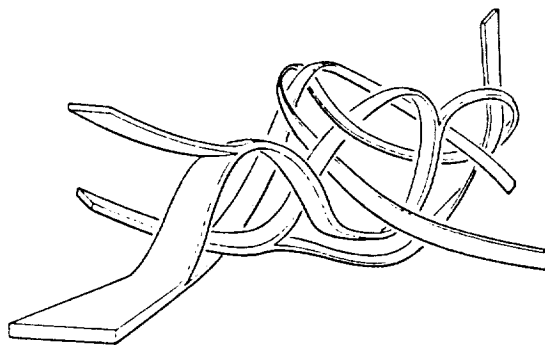
OXYGEN ATOM REFLECTOMETER FLOWN ON SHUTTLE STS-8

Atomic oxygen which does not react with a surface may accommodate to the surface or specularly scatter off the surface. Gregory performed an interesting experiment in space on STS-8 which gives some insight into these processes. Atomic oxygen was allowed to enter a slit in a short cylindrical segment which contained a silvered plastic strip to permit optical density measurements to determine the magnitude and direction of reactive species leaving a vitreous carbon target surface.



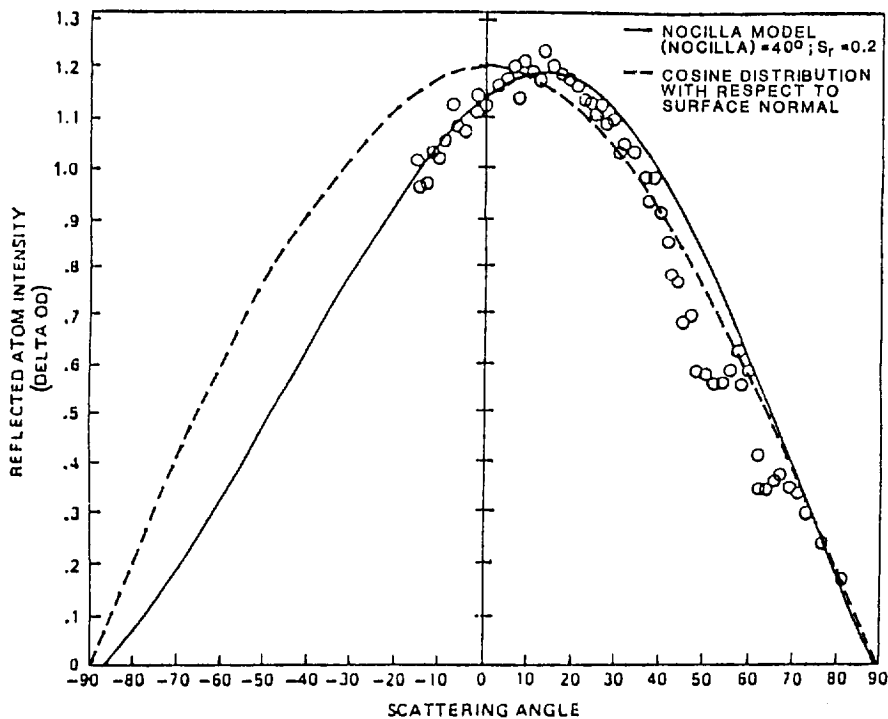
THE JENKINS MODEL OF THE STRUCTURE OF GLASSY CARBON

The vitreous carbon target used for this experiment does not have a preferential direction or plane because it is a woven tangle of graphine ribbons of random orientation.



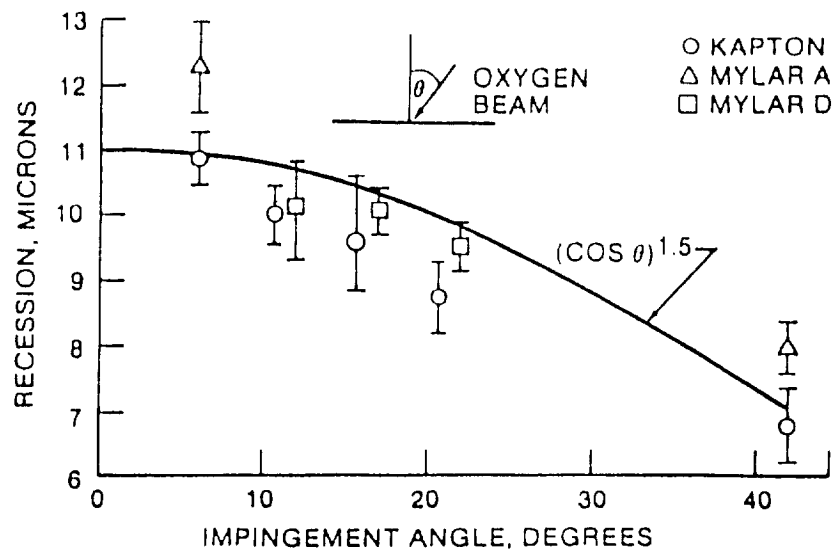
SCATTERED ATOMIC OXYGEN

Atoms of oxygen which do not react with the glassy carbon target surface appear to be ejected with a slight preferential forward specular scattering, indicating that at least a certain portion of the atoms do not totally accommodate to the surface. The facts that the ejection occurs at wide angles and that the probability of reaction is low on the first bounce contribute to a general concern that we must deal with atomic oxygen not only from the RAM direction, but from multiple bounce arrival to assure durability of reactive surfaces.



SURFACE RECESSION DEPENDENCE UPON ATOMIC OXYGEN IMPACT ANGLE

The angle of impact of the atomic oxygen affects the rate of surface erosion with an angular sensitivity proportional to the cosine of the angle with respect to the surface normal to the 1.5 power as opposed to the cosine to the 1 power, as would normally be expected. This may be an indicative that highly inclined surfaces may have a higher probability of specular scattering. The role that the microscopic cone formation on the surface plays with respect to this angular sensitivity is not clearly understood.



ATOMIC OXYGEN EROSION YIELD TEMPERATURE DEPENDENCE

Atomic oxygen erosion is a function of the temperature of a material as shown in this activation energy expression. The activation energies for several materials tested in space are shown on this chart.

$$\text{Erosion Yield} \propto e^{-\frac{\Delta E}{RT}}$$

ΔE = Activation Energy, calories/mole

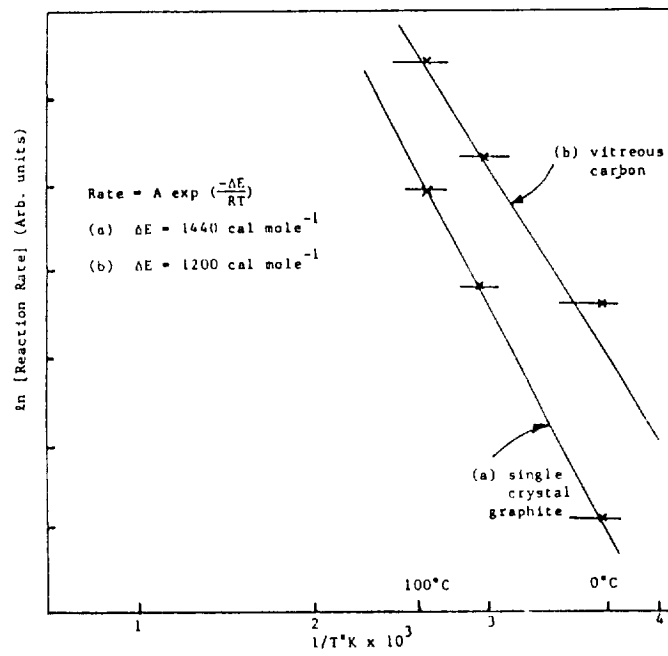
R = Gas Constant, 1.986 calories/(mole K)

T = Absolute Temperature, K

<u>MATERIAL</u>	<u>ACTIVATION ENERGY ΔE, CALORIES/MOLE</u>
Vitreous carbon	1,200
Graphite	1,400
CR-39 (bisallyl diglycol carbonate, an optical plastic)	1,050

EFFECT OF TEMPERATURE ON OXIDATION RATE OF CARBON ON STS-8

Heated vitreous carbon and single crystal graphite samples on STS-8 were used to make an Arrhenius plot to determine the activation energies for these materials.



POLYMERIC FILMS AT VARIOUS TEMPERATURES ON STS-8

Efforts to measure the effect of sample temperature on erosion yield of Kapton, Mylar A, Mylar D, and clear Tedlar on STS-8 have not resulted in the discovery of measurable dependencies greater than the uncertainty of the temperatures used for the experiment.

MATERIAL	THICKNESS, μm (MILS)	EXPOSED SIDE	SURFACE RECESSION, μm	
			STRIP SAMPLES	
			121° C	65° C
KAPTON	12.7 (0.5)	AIR ROLL	9.5	10.5
			11.8	10.3
KAPTON	25.4 (1.0)	AIR ROLL	9.8	10.7
			9.9	9.0
KAPTON	50.8 (2.0)	AIR ROLL	11.1	10.6
			11.1	11.1
MYLAR A	12.7 (0.5)	AIR	12.7	12.3
MYLAR A	40.6 (1.6)	AIR	12.1	11.9
MYLAR D	50.8 (2.0)	AIR ROLL	9.9	10.2
			11.0	10.4
CLEAR TEDLAR	12.7 (0.5)	AIR	10.9	11.5

ACTIVATION ENERGY, ΔE , CALORIES/MOLE

This table compares activation energies calculated from space experiments with laboratory experiments performed by various researchers. The data may suggest that the level of understanding of activation of energies in space and in the laboratory simulation of space is rather low. However, data obtained in ground experiments occasionally are consistent with the results obtained in space experiments.

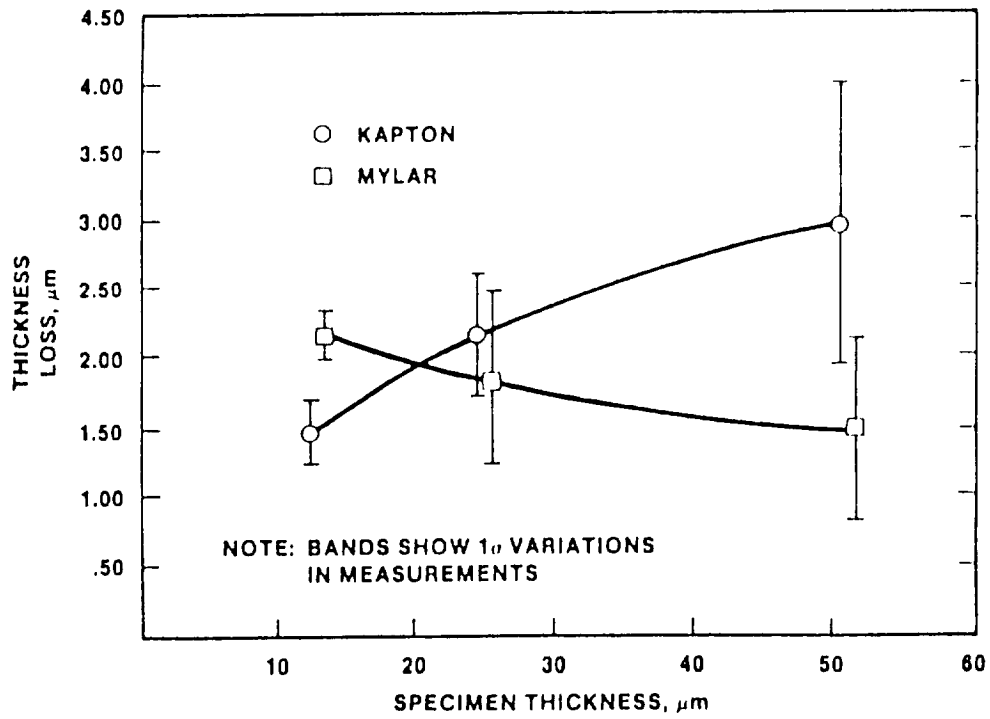
<u>MATERIAL</u>	<u>SPACE</u>	<u>LABORATORY</u>
Graphite	1400 ^A	2300 ^C 3580 ^D 1437 ^E
Kapton H	72 ^B	
Kapton HN		1325 ^F
FEP	Indeterminate ^B	369

SOURCES:

- A-J. Gregory, STS-8
- B-J. Visintine, STS-8
- C-C. Park
- D-G. Arnold and D. Peplinski-1ev
- E-S. Rutledge - RF Asher

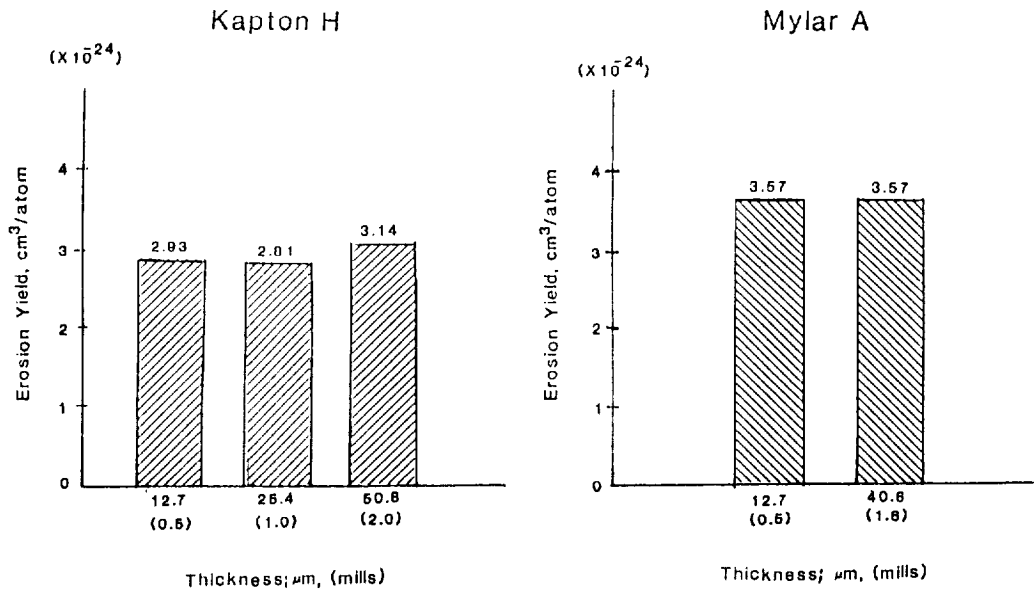
ATOMIC OXYGEN EROSION DEPENDENCE UPON POLYMER FILM THICKNESS (STS-5)

Measurements taken on STS-5 indicate a slight erosion yield dependence of polymer thickness on Kapton and Mylar.



EROSION YIELDS AS A FUNCTION OF POLYMER FILM THICKNESS (STS-8)

Measurements taken on STS-8 indicate a far smaller sensitivity to polymer film thickness than was previously observed on STS-5. Film thickness may play an indirect role because of film processing materials which may be present on the surface of polymers to varying degrees depending upon the thickness of the specific polymer. Such surface contaminants may act as atomic oxygen barriers until sufficiently large fluences remove them.



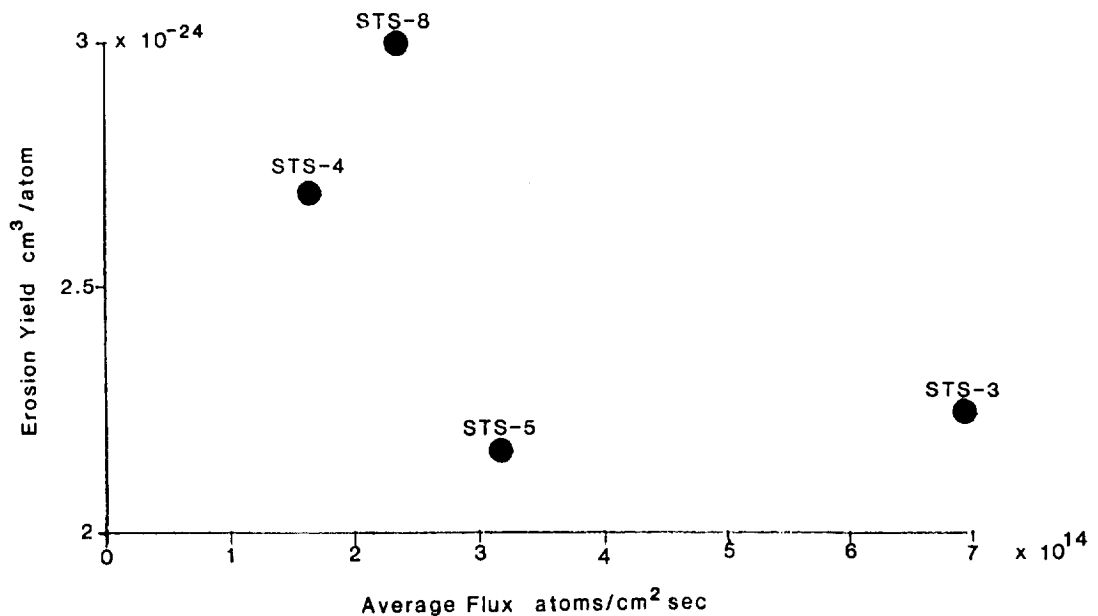
EFFECT OF SOLAR RADIATION ON EROSION YIELD

The question of whether or not atomic oxygen is synergistically affected by solar radiation has been addressed, with the resulting conclusion that if there is any effect, it is very small, and not within measurable significance for the data taken to date. If one assumes graphite is a material whose erosion yield is independent of solar radiation effects, then one finds most of the polymers have erosion yields in the sun which are lower than in the dark. However, if one makes calculations based on fluence estimates, the ratio of erosion yield in the day to erosion yield at night appears to close to 1 or slightly positive, indicating that there may be some slight synergistic effect, but of questionable magnitude relative to the uncertainty.

<u>MATERIAL</u>	<u>DAY EROSION YIELD</u> <u>NIGHT EROSION YIELD</u>	<u>ASSUMING GRAPHITE REACTIVITY</u> <u>IS INDEPENDENT OF SOLAR RADIATION EFFECTS</u>	<u>BASED ON</u> <u>FLUENCE ESTIMATES</u>
Graphite	=	1.0	1.2-1.7
Polyethylene		0.8	0.9-1.3
Kapton H		.9	1.0-1.5
Mylar A		.9	1.0-1.5
Kapton F		Indeterminate	Indeterminate

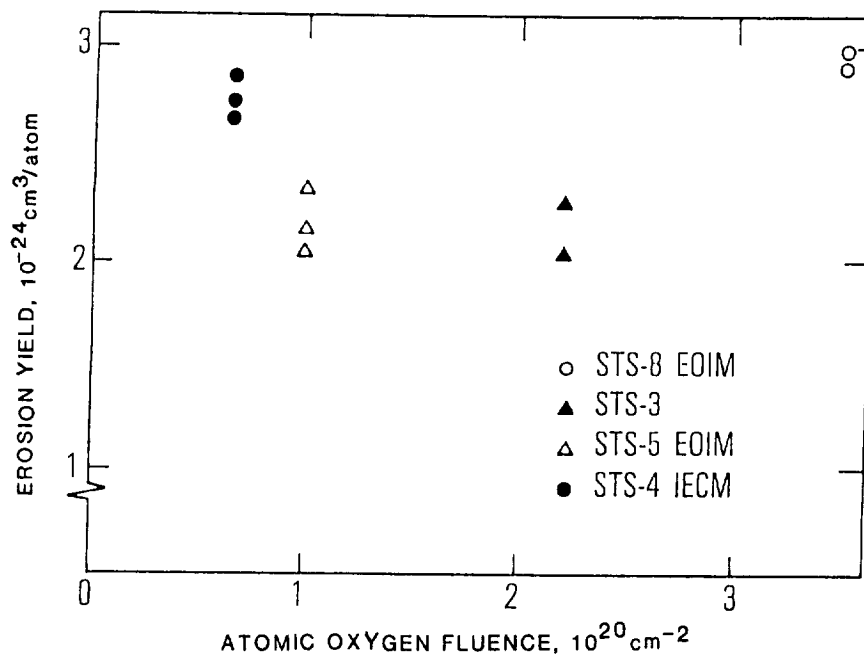
ATOMIC OXYGEN EROSION YIELD FOR KAPTON H AS A FUNCTION OF FLUX

One can make a plot of the erosion yield versus the average flux for several of the STS flight experiments to find that there is significant data scatter, but that some trend of reduced erosion yield as a function of increasing flux can be observed. However, it is very difficult to draw any definite conclusion because the average flux may be the result of averaging a high flux and near zero flux and comparing that with a moderate flux from another flight. One can make arguments that erosion yield should increase with flux due to interaction of radicals and metastables with each other, and also that erosion yield should decrease with increasing flux due to increases in nonreactive scattering of the incident atomic oxygen upon oxygen resident at the surface. The effects of RAM versus sweeping atomic oxygen impingement may also contribute to difficulty in data interpretation.



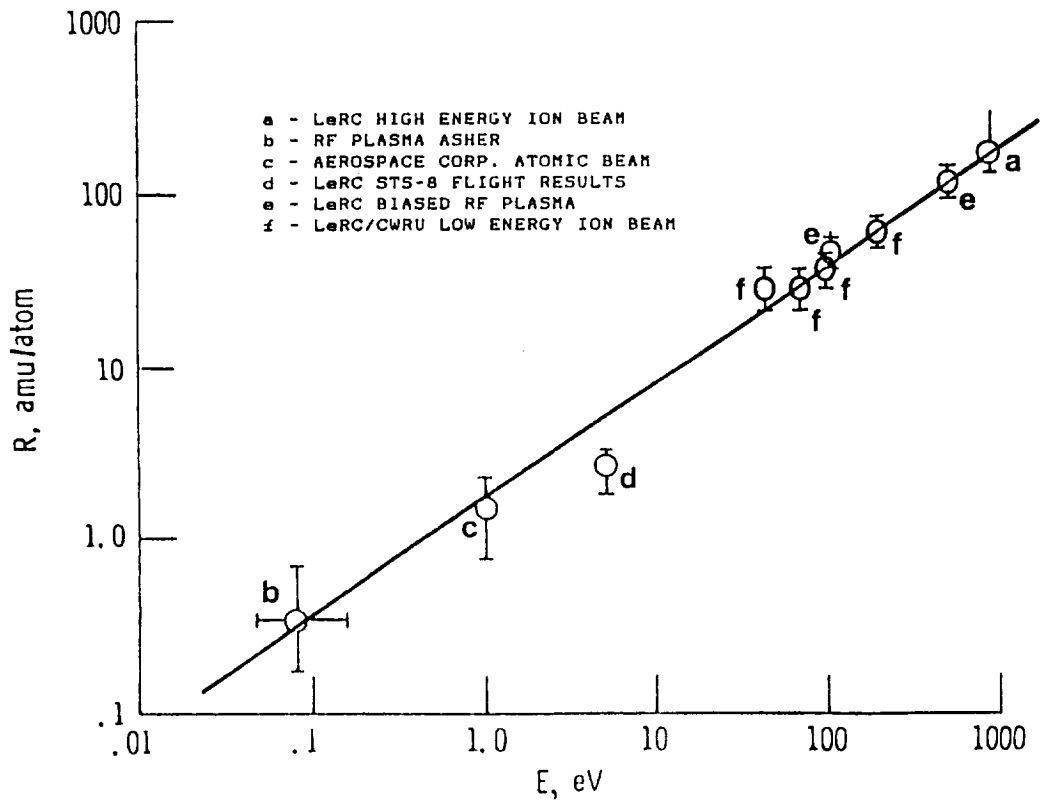
EROSION YIELD OF KAPTON H AS A FUNCTION OF ATOMIC OXYGEN FLUENCE

Erosion yield sensitivity to fluence is also widely scattered, indicating no clear trend. In the case of erosion yield fluence dependence, one could make argument that induction mechanisms may cause erosion yield to increase once a certain level of polymeric degradation is achieved by virtue of the arrival of a sufficiently high fluence.



KAPTON MASS LOSS RATES VS. OXYGEN ENERGY

The erosion yield may also be dependent upon energy, as shown in this plot, which combines space data with low energy thermal asher data and high energy ion beam data. As one can see, there appears to be a very definite increase in the yield with kinetic energy.



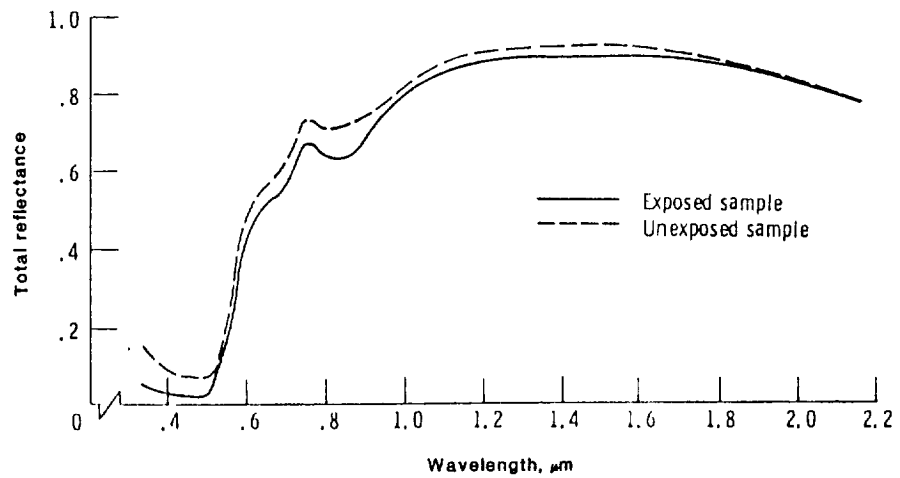
DEPENDENCE OF EROSION YIELD ON PRESENCE OF ATMOSPHERIC OXYGEN IONS

The dependence of erosion yield on whether or not oxygen is charged has been addressed by Gregory using carbon, and by Gull using osmium. Because the charge population of atomic oxygen is so low in low Earth orbit, one would not expect to see any measurable dependence. Although no effect was seen on STS-8, the question is very relevant with respect to simulation systems where either ions or neutrals may be chosen for low Earth orbital simulation.

- . No measurable effect on STS-8
- . LEO ionic oxygen population too low ($\frac{Q^+}{O} \sim 10^{-4}$)
to measure a dependence

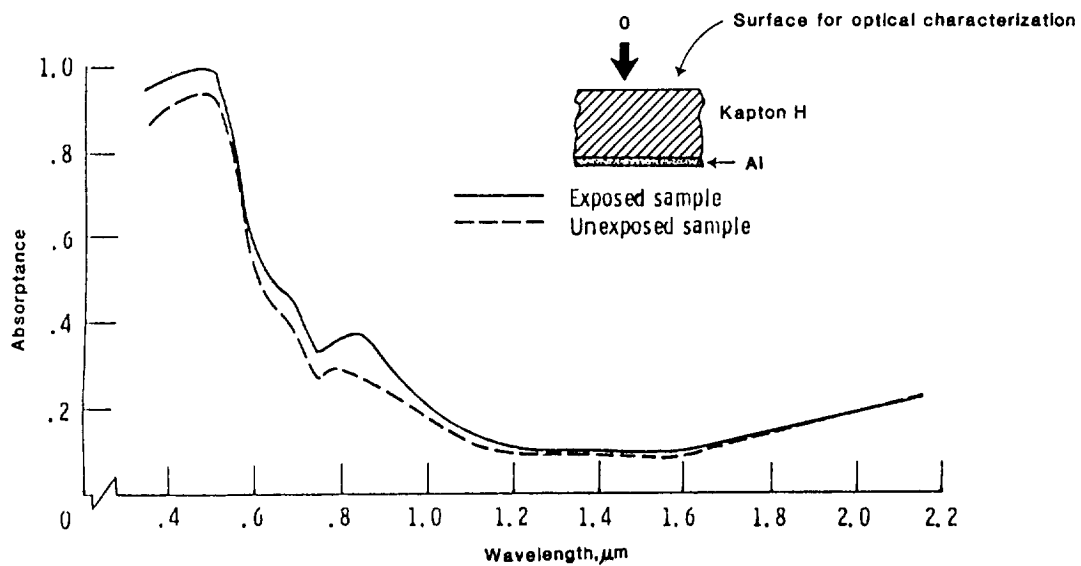
EFFECT OF ATOMIC OXYGEN ON TOTAL REFLECTANCE OF BACK ALUMINIZED KAPTON H (STS-8)

Polyimide Kapton H shows only a slight reduction in total reflectance as a result of atomic oxygen exposure.



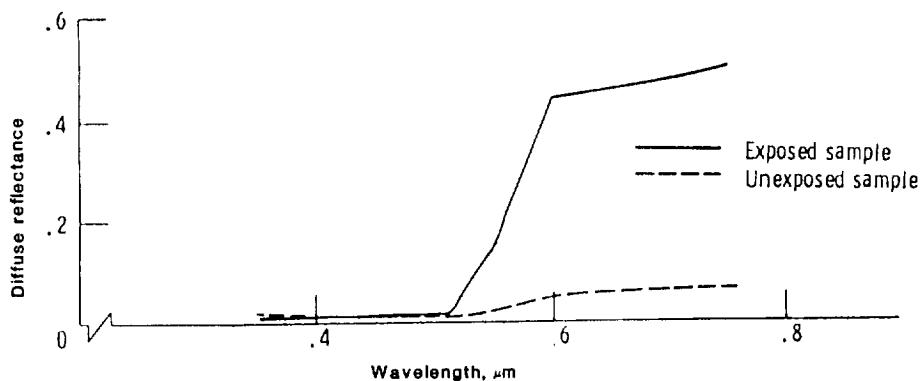
EFFECT OF ATOMIC OXYGEN ON ABSORPTANCE OF BACK ALUMINIZED KAPTON H
(STS-8, FLUENCE = 3.5×10^{20} atoms/cm²)

Similarly, there is a slight increase in absorptance as a result of atomic oxygen exposure. Much of this may be due to the fine cone-like structures on the surface contributing to a slight reduction in reflectance and an increase in absorptance.



EFFECT OF ATOMIC OXYGEN ON DIFFUSE REFLECTANCE OF BACK ALUMINIZED KAPTON H (STS-8)

The dominant optical change for Kapton and all polymers is the optical consequence of the microscopic surface structures contributing substantially to the diffuse reflectance and subsequent reduction in specular reflectance. It is the increase in diffuse reflectance that makes all the polymer surfaces appear matte-like and diffuse with respect to transmittance as well as reflectance.



EFFECT OF LEO ATOMIC OXYGEN ON OPTICAL PROPERTIES OF MATERIALS

The changes in solar absorptance and reflectance of various materials are listed in this table. As can be seen, the most significant changes occur for those materials which allow organic surfaces to be exposed to atomic oxygen. Thermal blanket materials such as aluminized Kapton or aluminized FEP Teflon display changes in solar absorptance and thermal emittance which would alter their performance as thermal blankets or radiator materials.

<u>Material</u>	<u>Change in Optical Properties due to A/O</u>		
	<u>Solar</u> <u>Absorptance</u>	<u>Emittance</u>	<u>Reflectance</u>
Kapton H (aluminized)	0.041	-	-0.051
Urethane (black, conductive)	0.042	0.55	-
Z853, yellow	-0.34	-	-
Chemglaze Z302 (glossy, black)	0.011	-	-0.01
Chemglaze A276 (white)	-0.005	0.03	-0.039
Silicone RTV-670	-0.004	-	0.001
Silicone (black, conductive)	0.0	-0.005	-
GSFC (green)	-0.002	-	-
Aluminum (150 Å)	0.0	0.0	0.0
SiO ₂ (650 Å on Kapton H)	0.0	0.0	0.0
Silicone RTV-650+TiO ₂	0.001	-0.01	-
Aluminum (chromic acid oxidized)	0.0	0.0	0.0
AlMgF ₂	-	-	0.0
Silicone S1023	-0.022	-0.02	-
Chemglaze A276 (w/modifiers)	-0.006 to 0.016	0.02	-
Chromium (123 Å)	0.0	0.0	0.0

<u>Material</u>	<u>Change in Optical Properties due to A/O Solar</u>		
	<u>Absorptance</u>	<u>Emittance</u>	<u>Reflectance</u>
Al ₂ O ₃	0.0	-	0.0
Silicate MS-74	0.01	0.0	-
Urethane inhib A-276	0.0	0.01	-
FEP Teflon with silver undercoat	0.006	0.0	-
Bostic 463-14	0.01	0.0	-
Indium Tin Oxide coated Kapton H with aluminized backing	0.006	0.004	-
Kapton with aluminized backing	0.048	0.018	-
Nickel	0.005	0.0	-
Polyurethane A-276	0.023	0.01	-
Silicone RTV-602/Z302	-0.004	-	-
S13 - GL0	-0.005	0.0	-
YB-71	0.005	0.0	-
Z306 (flat black)	-0.022	0.0	-
Black, carbon-filled PTFE impregnated fiberglass (0.127 mm thick)	-0.16	-0.05	-
Aluminized Kapton, second surface mirror, uncoated (0.052 mm thick)	-0.23	-0.59	-
Aluminized FEP Teflon, second surface mirror (0.025 mm thick)	0.05	-0.19	-
Siloxane coating, RTV 602/ 0 on aluminized Kapton, second sur- face mirror substrate (0.008 mm thick coating) (0.052 mm thick Kapton)	0.0	0.0	-

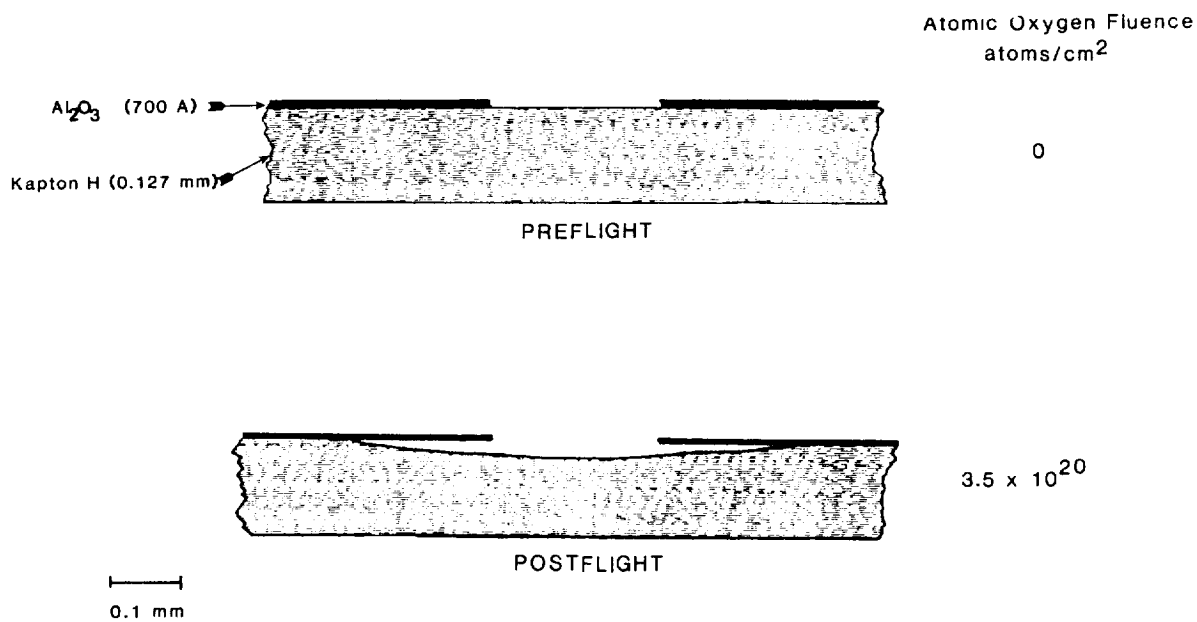
DIMENSIONAL CHANGES DUE TO ATOMIC OXYGEN REACTION

Atomic oxygen may cause dimensional changes in either the surface or the bulk of some materials. In the case of silver, a slight oxidation can be tolerated. However, significant oxidation with diffusion into the bulk causes the formation of an oxide which expands and does not remain adherent to the unreacted silver. In the case of silicone, the bombarded surface tends to form silicon dioxide with the loss of surface organic groups so that surface contraction and cracking occurs. Depending on the thickness of the silicone, underlying organic material below the coating may become exposed to atomic oxygen.

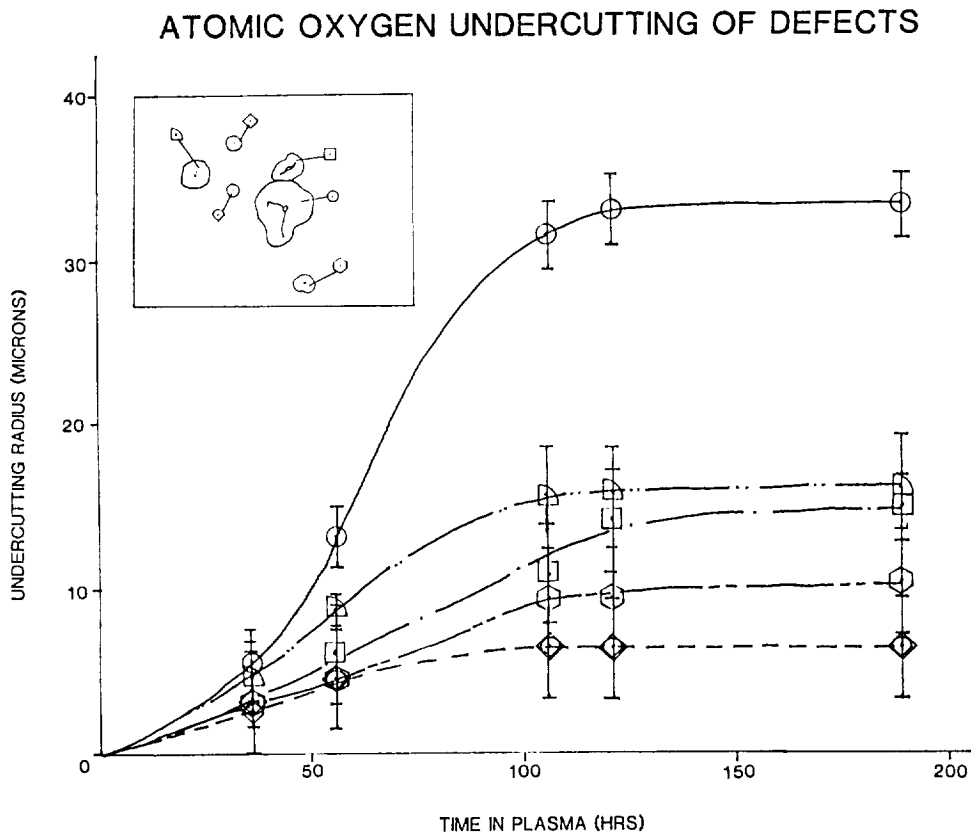
- Silver + O → Silver Oxide (expansion + spalling)
- Silicone + O → Surface Oxidation (contraction + cracking)

ATOMIC OXYGEN UNDERCUTTING - STS-8

Atomic oxygen undercutting has been observed in samples on STS-8 as shown in this scale drawing of a cross section of a defect which was initially on the surface prior to atomic oxygen exposure in space. The wide undercutting could be a problem depending on the population density of surface defects, whether caused by fabrication procedures, handling, micrometeoroids, or debris.

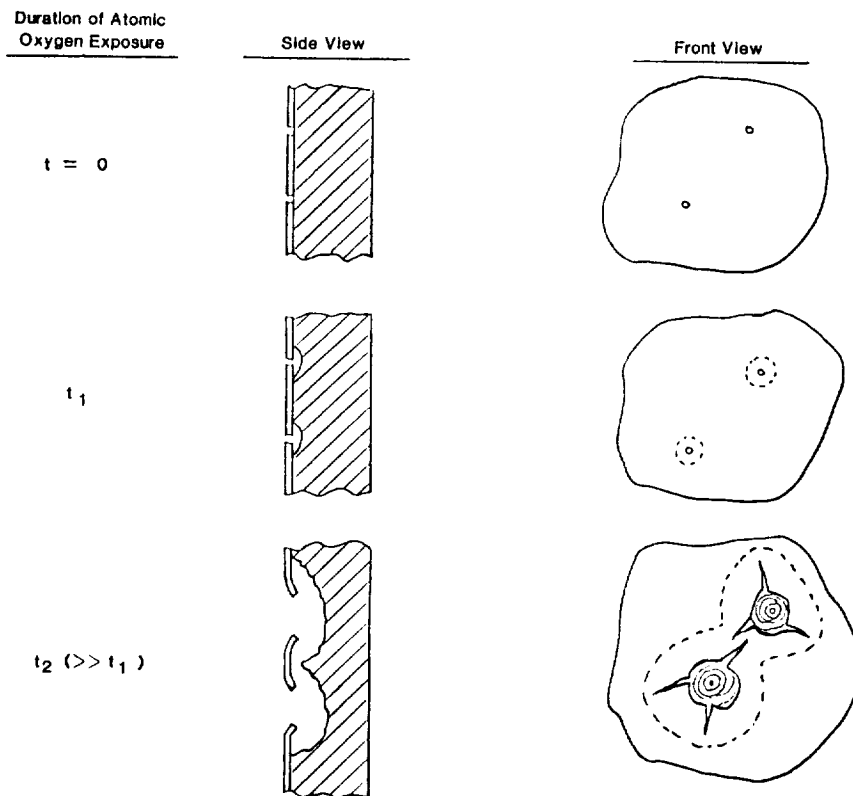


Measurement for defects in thin film protective coatings over polyimide Kapton have disclosed approximately 22,000 atomic oxygen transparent defects per square centimeter. If undercutting occurs without end, bulk failure of tensile-loaded polymeric blankets would eventually occur. However, as can be seen in this plot, in simulation tests performed in laboratory plasma ashers, undercutting tends to terminate. Thus, the survivability of atomic oxygen protective coatings may perhaps more depend on defect density than the fluence.



PROTECTIVE COATING FAILURE MODE

This viewgraph depicts the observed atomic oxygen undercutting failure scenario which occurs if the thin-film protective coating tears as the undercutting increases. Thus, not only is it necessary to control the defect density within limitations, but the nature of the coating must be such that tearing does not occur, even though undercutting may self-limit.



SUMMARY

Understanding of the basic processes of atomic oxygen interaction is currently at a very elementary level. However, measurement of erosion yields, surface morphology, and optical properties for low fluences have brought about much progress in the past decade. Understanding the mechanisms and those factors that are important for proper simulation of low Earth orbit is at a much lower level of understanding. The ability to use laboratory simulations with confidence to quantitatively address the functional performance and durability of materials in low Earth orbit will be necessary to assure long-term survivability to the natural space environment.